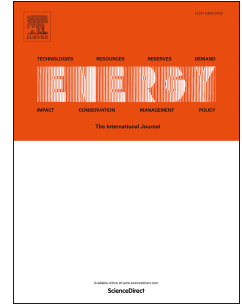


Accepted Manuscript

The design, construction and experimental characterization of a novel concentrating photovoltaic/daylighting window for green building roof

Qingdong Xuan, Guiqiang Li, Yashun Lu, Bin Zhao, Xudong Zhao, Gang Pei



PII: S0360-5442(19)30551-1

DOI: <https://doi.org/10.1016/j.energy.2019.03.135>

Reference: EGY 14971

To appear in: *Energy*

Received Date: 27 December 2018

Revised Date: 14 March 2019

Accepted Date: 24 March 2019

Please cite this article as: Xuan Q, Li G, Lu Y, Zhao B, Zhao X, Pei G, The design, construction and experimental characterization of a novel concentrating photovoltaic/daylighting window for green building roof, *Energy* (2019), doi: <https://doi.org/10.1016/j.energy.2019.03.135>.

This is a PDF file of an unedited manuscript that has been accepted for publication. As a service to our customers we are providing this early version of the manuscript. The manuscript will undergo copyediting, typesetting, and review of the resulting proof before it is published in its final form. Please note that during the production process errors may be discovered which could affect the content, and all legal disclaimers that apply to the journal pertain.

This work is licensed under a Creative Commons Attribution-NonCommercial-NoDerivatives 4.0 International License.

**The design, construction and experimental characterization of a
novel concentrating photovoltaic/daylighting window for green
building roof**

Qingdong Xuan¹, Guiqiang Li^{2*}, Yashun Lu¹, Bin Zhao¹, Xudong Zhao², Gang Pei^{1*}

¹ *Department of Thermal Science and Energy Engineering, University of Science and
Technology of China, 96 Jinzhai Road, Hefei City 230026, China*

² *School of Engineering, University of Hull, Hull HU6 7RX, UK*

*Corresponding authors. Tel/Fax: +86 551 63607367. E-mail: guiqiang.li@hull.ac.uk;
peigang@ustc.edu.cn.

Abstract: A novel concentrating photovoltaic/daylighting window to achieve the multi-function of the electricity generation and daylighting for buildings has been designed, constructed and experimentally characterized. It's found that the concentrating photovoltaic/daylighting window can achieve a transmittance of around 10% for the natural daylight without decreasing the optical efficiency of the concentrator. The overall daylighting and electrical performance of the concentrating photovoltaic/daylighting window are investigated under the real weather condition. The hourly illuminance level, the temperature of the inner environment of the box and transient I–V curves are determined. The short-circuit current, open-circuit voltage maximum power generation, and Fill Factor of the system are derived from each individual I–V curve. Through the experiment testing, the illuminance level in the integrating box is in the range of 923-9230 lx with the outside illuminance level exceeds 100000 lx during noon time, which prove that the concentrating photovoltaic/daylighting window can improve the visual comfort for the building

interior environment and it can also avoid the building interior environment from overheating and dazzling at noon which is caused by direct sunlight through transparent window. The preliminary economic analysis of the new concentrating photovoltaic/daylighting window is also made.

Keywords: concentrating photovoltaic/daylighting window; outdoor experiment; illumination; daylighting performance; electrical performance

1. Introduction

Speaking of the energy resource structure today, fossil fuels, such as petroleum, coal and natural gas etc., still account for more than 90% of the world total energy demand. The drawbacks of the vast use of the fossil fuels are obvious, the most serious one is the release of the greenhouse gas most composed of carbon dioxide (CO₂). The main concern towards the increasing level of CO₂ and other greenhouse gas in the atmosphere is the global climate change. It has been reported that the share of the building energy consumption takes more than 40% of the total energy demand in developed countries and is still in increasing trend. For developing countries, this value is less, but with the growth of the population, urbanization, and demands of building services and comfort levels, the sharp rise of building energy use is probably inevitable [1]. It was estimated by the Energy Information Administration (EIA) that the consumption of the electricity for lighting for the residential and commercial sectors in 2016 is 279 billion kWh, which was around 10% of the total electricity consumption by these sectors and around 7% of the total electricity consumption in the United States [2]. As the growing of the population, the building construction area will experience a sharp growth in the next decades, which will lead to the sharp increase of the energy consumption in the building sectors includes the need for lighting. However with an appropriate daylighting design, about 40% lighting energy could be saved [3]. In this regards, it's necessary to encourage the renewable energy utilization technology to be considered into buildings by the combination of the functions of the electricity generation and natural daylighting.

Solar energy as a kind of clean and inexhaustible energy resource which is widely used in many fields (for example, producing the drinking water through evaporation–condensation processes [4]) would be suitable to be used on buildings for most buildings are exposed to the solar radiation. Technologies that introducing the solar energy into buildings are usually Building integrated photovoltaic (BIPV) or building attached photovoltaic (BAPV) systems [5]. The International Energy Agency (IEA) predicted that BIPV technology considered during the design and construction of all kinds of buildings are likely to be a future potential [6]. As it was predicted by an IEA report about the prospect of the BIPV systems in 14 selected countries, the total potential area of BIPV systems can reach around 23 billion m² which is able to generate the electricity of 3 pWh annually [7]. It was concluded by Oliver and Jackson that compared with the centralized PV plant, BIPV systems possess three main benefits [8]:

- (1) The need of the land, fence, access road and other important support components can be avoided, for the PV panels are attached or replacing the building structure. The most buildings are close to the electricity grid which means that some cabling cost can also be avoided;
- (2) When the electricity is generated by the BIPV systems, it will be consumed by buildings themselves, therefore the losses that caused by the transmission and distribution of the electricity can be minimized. What's more, for the commercial buildings, their electricity demands coincide with the peak electricity generation from BIPV systems;

(3) The overall cost of the BIPV system can be further reduced due to the substitution parts of the building roof, window and façade.

At present, it was highlighted by many researchers that introducing the concentrating device into the concept of BIPV as the BICPV (Building Integrated Concentrating Photovoltaic) has many advantages, because with the use of the concentrator, it can reduce the PV material and provide higher heat resource. Even at the present situation when the cost of PV cells decrease continuously and increase in their efficiency [9], the cost and environmental advantage of the low concentration PV or PV/T systems for BI (Building Integrated) application are still obvious [10]. So the use of the concentrators have significantly increased in the last decades, such as sky lights, double glazing windows and solar blinds [11]. The concentrator is a device that usually makes use of geometrical optics in the design of reflective and/ or refractive types of concentrating devices to focus the solar flux onto a receiver module where the PV cell is attached [12, 13]. In this area, the compound parabolic concentrator (CPC) is proved to be a more utility and economic one [14], which was first invented in the U.S. in 1970s [15, 16].

Since the concept of the CPV proposed for the BIPV systems, a lot of researchers dedicated into inspiring the use of the compound parabolic concentrator and its optimization structure on buildings. Carlo Renno et al designed a concentrating PV/Thermal system based on the CPC that can provide the electricity for the domestic use and recover the solar cell thermal energy to both supply heat for the domestic use and enhance the PV performance at the same time [17]. Mallick et al designed a novel

asymmetric CPC which consists of two asymmetric compound parabolic curves, and the simulation and experiment results showed that it is feasible to be used on the building façade at Northern Ireland ($54^{\circ}36'N$, $5^{\circ}37'W$). Experiment results indicated that the asymmetric mirror CPC (with geometric concentration ratio of 2.0X) increased the PV power by 62% and that was 101% for a dielectric asymmetric CPC (with geometric concentration ratio of 2.45X) [18, 19]. Used the same asymmetric structure, Lu et al. integrated the PCM material with Building Façade Integrated Asymmetric Compound Parabolic Photovoltaic concentrator (BFI-ACP-PV) system, and an increase of 5% for the PV conversion efficiency was achieved [20].

It's worth noting that the lens-walled CPC as an optimization structure from the traditional CPC (which was first invented by Su et al. [21]), is drawing more and more attention. Li et al. performed the optical simulation for the optimization of the lens-walled structure during the design stage [22] and analyzed its flux distribution on the receiver as compared with the traditional mirror CPC [23]. The design of the lens-walled structure is to use the refraction to enlarge the acceptance range of the concentrator but reduce the material needed thus to reduce overall cost and weight of the system. To enhance the optical performance of the concentrator, Li et al. proposed the air-gap lens-walled CPC by setting an air gap between the lens structure and the mirror reflectors which adopted both the total internal reflection and the specular reflection to collect sun rays [24]. Simulation and experiment study indicated that the air-gap lens-walled CPC can increase the optical efficiency by more than 10%. In addition, they further built a CPV/T system based on the air-gap lens-walled CPC [25],

and conducted both numerical simulation [26] and experiment [27] study about this system. As for the building south wall integration, Xuan et al. pointed out that the concentrator in asymmetric structure might be a better choice [28], so they designed an asymmetric lens-walled CPC which is proved to have a large acceptance range up to 60° with high optical efficiency [29, 30]. In conclusion, the advantages of the lens-walled CPC are: large acceptance range that makes it suitable for building south integration without additional tracking components or seasonal adjustment; high optical efficiency; uniform flux distribution on the receiver and less material used thus to reduce the overall cost and weight of the system.

Another advantage of using concentrators for the building integrated solar energy utilization systems is that the concentrator itself can act as the support structure for the whole system. So the construction of zero net energy related buildings would be easier and cheaper, and the use of high transmittance optical material makes the concentrating PV devices better suited into buildings thus present better artistry. What's more, the use of high transmittance material for the concentrator would also inspire the design imagination of the multi-function concentrating solar systems such as CPV/D and CPV/T/D (Concentrating Photovoltaic/Thermal/Daylighting). The traditional flat PV systems will block sun rays from entering the room, which makes it unlikely or inefficient to add the function of daylighting. On the contrary, the concentrator can change the direction of sun rays and sun rays escape is a common issue for the concentrator, so it would be feasible to redirect these sun rays into the building for daylighting. Feng et al. proposed a novel CPV/T/D system based on the

dielectric CPC (which is filled with PMMA). The working principle of this CPV/T/D system is to collect sun rays for electricity generation within the acceptance range of the dielectric CPC, while when the incidence angles of sun rays exceed the acceptance range, sun rays will escape into the building for daylighting [31]. As the bigger incidence angles usually occurs in the morning or evening, so the CPV/T/D system is likely to achieve the self-adoption indoor daylighting control [32]. The parametric study by CFD simulations has shown that different design parameters had obvious effects on the actual performance of the CPV/T/D system [33]. However, for the CPV/T/D system, the change of the distribution percentage of the incoming solar radiation for daylighting and PV is in Ramsay Rule, which means that when the system works at the electricity-generation condition, very few energy can reach into the building for daylighting and vice versa. Shanks et al. presented a novel concentrator photovoltaic (CPV) system embedded as a window for electricity generation and daylighting based on the crossed compound parabolic concentrator (CCPC) [34].

In the previous study, Li et al. proposed a novel use of the lens-walled CPC by setting a “daylighting window” near the base area to combine the functions of the renewable electricity generation and the natural daylighting together [35], but in that study, only the preliminary feasibility analysis of the multi-function of the CPV/D module and the structure optimization analysis for the concentrator has been provided through the optical simulation. The research work before mainly focused on the total energy captured by the CPV/D module, i.e. the distribution percentage of the total

energy that can be used for daylighting and the distribution percentage of the total energy that can be used for the electricity generation at various incidence angles. In other words, the previous study still mostly concentrated on the concentrator itself, and the optical simulation study was conducted to prove the feasibility of the symmetric lens-walled CPC to achieve the multifunction of the electricity generation and daylighting. However the actual illumination condition of the interior environment and the concentrating PV performance under the coupled working condition of the electricity generation and the natural daylighting are more important for the CPV/D window but not involved in the previous study. Especially for the daylighting performance, the determination of the illuminance level of the interior room by adopting this kind of CPV/D window is very important for the reference of the practical engineering. Besides, due to the sun motion, the solar altitude angle and azimuth angle change throughout the day, which makes the actual solar incidence angle for the CPV/D module much different from the incidence angle of the projection of the sun ray on the North-South vertical plane, which would finally have a significant effect on the actual performance of the CPV/D window. This paper aims to bridge this gap and carry out a descriptive experimental study and analysis on the real time operation of the CPV/D window.

Therefore in this paper, based on the optimized concentrator structure, the prototype of the CPV/D window is manufactured, assembled and integrated with the integrating box. The actual illumination condition of the interior environment and the concentrating PV performance under the coupled working condition of the electricity

generation and the natural daylighting are investigated. The actual daylighting and electrical performance of the CPV/D window is identified every 20 minutes from 8:40 to 17:20. The temperature of the PV panel and inner environment of the experiment box was collected by the T-type thermocouples through the data logger. The detailed illuminance level in the box and electrical performance of the CPV panel were determined. The preliminary cost assessment for the concentrator is also made for the CPV/D window.

2. Design and preliminary function analysis of the concentrating photovoltaic/daylighting (CPV/D) system

As illustrated in Fig.1 is the key component of the concentrating photovoltaic/daylighting (CPV/D) system, the main structure of which is the lens-walled compound parabolic concentrator (CPC). Fig.1 (a) shows the working principle of the lens-walled CPC that acts both as the concentrating device to focus the incoming solar radiation onto the receiver where the PV cell is attached to generate the electricity and as the “daylighting window” to redirect the sunrays into the room for daylighting to achieve a better energy partition balance. The formation process of the lens-walled structure can be described as: the outer contour AB and CD are traditional symmetric compound parabolic curves. The lens-walled structure is shaped up by rotating AB and CD by the up end points A and C with a certain angle (usually $3-5^\circ$). The outer surface of the lens-walled CPC is coated with the aluminum film to collect the solar radiation through the specular reflection but leaving the lower part around the base area uncoated to set the “daylighting window” which can allow the sun rays to get into the room. In this way, the concentrator can achieve dual functions of the electricity

generation and daylighting to form the multifunctional concentrating photovoltaic/daylighting window.

The prototype of the CPV/D module is shown in Fig. 1 (b), which is made of the polymethyl methacrylate (PMMA). The evaporated aluminum coating technology is employed to process the mirror reflectors (with the specular reflectivity of around 85%), and as interpreted in the last section, leaving the outer surface near the base area uncoated to access the “daylighting window”.

Here may arouse the concern towards the optical efficiency (the ratio of the solar energy captured by the receiver to the total incoming solar energy through the front aperture) of the proposed concentrator for all outer surface of the traditional concentrator is all designed as the reflection surface to concentrate the solar radiation. Before the outdoor experiment, the ray-tracing simulation is conducted to predict the optical and daylighting performance of the CPV/D module. The indoor experiment under the solar simulator was conducted to verify the ray-tracing simulation results. It's worth noting that for the design of the optical concentrator, the ray-tracing simulation through the software is a key stage [29]. Many researchers such as Nazmi Sellami et al. [36], Imhamed M. et al. [37], Firdaus MuhammadSukki et al. [38], Daniel Chemisana et al. [39], Zheng et al. [40] and Su et al. [41] have performed the optical simulation to design and optimize the concentrators and studied the optical performance of them before the experimental study. The research experience of them proved that optical simulation by all kinds of software is a fast, efficient, accurate and cheap way of

designing, optimizing and study the optical performance of the concentrator which is also accepted worldwide.

The simulation η_{opt} and experiment $\eta_{opt,ac}$ optical efficiency as well as the daylighting efficiency $\eta_{daylighting}$ at various incidence angles are presented in Fig. 2. The experiments are conducted indoor at the standard test condition (STC) under a solar simulator from Newport Corporation (Oriel Sol3A Model 90943A). Through the comparison of the simulation and experiment results, it can be concluded that for the holistic-coating lens-walled CPC, the actual optical efficiencies are basically consistent with the simulation ones at various incidence angles despite some inevitable deviations caused by manufacture errors, mismatch losses and series resistance losses, etc. [26]. Thus prediction results from the ray-tracing simulation are convincing.

$$\eta_{opt} = \frac{Q_{PV}}{Q_{Total}} \quad (1)$$

$$\eta_{opt,ac} = \frac{1}{C} \frac{I_{sc}^{with}}{I_{sc}^{without}} \quad (2)$$

$$\eta_{daylighting} = \frac{Q_{Daylighting}}{Q_{Total}} \quad (3)$$

Where Q_{PV} is the total solar irradiation captured by the PV cell; Q_{Total} is the total incoming solar radiation from the front aperture; $Q_{Daylighting}$ is the solar radiation for daylighting; I_{sc}^{with} is the short circuit current of the concentrating PV; $I_{sc}^{without}$ is the short circuit of the non-concentrating PV) to identify the actual performance of the concentrator. C is the geometric concentration ratio.

It can be seen clearly from the ray-tracing simulation results as shown in Fig. 2 that for the lens-walled CPC with holistic coating on the outer surface and non-coated

at the base area to set the “daylighting window”, the optical efficiencies of them at various incidence angles are almost at the same level which can dispel the concern about the optical efficiency, because it can be predicted that the CPV/D module only uses escape sunrays for daylighting that won’t reduce the total energy captured by the PV cell but increase the solar energy usage ratio. The daylighting efficiency of the CPV/D module within the acceptance range of the 2.4X lens-walled CPC (around 30°) remains at around 10%, while once the incidence angle is larger than the acceptance range, the daylighting efficiency exceeds to around 78% (Fig. 2). It should be noted that, the larger incidence angles for the symmetric concentrator in east-west orientation usually occurs in the early morning and later afternoon when the solar radiation is weak, so the CPV/D module may have the function of the daylighting control in the room. The ray-tracing simulation far from above is the only preliminary confirmation of setting the “daylighting window” near the base area won’t decrease the optical efficiency of the concentrator.

3. The outdoor experimental characterization system

3.1 The design and construction of the CPV/D experimental system

3.1.1 Concentrator construction

The key component of the CPV/D system, i.e. lens-walled compound parabolic concentrator is manufactured using CNC wire cutting technology and then, the concentrators are polished to make it transparent again to maintain a high transmittance. The material is selected as PMMA, which is proved to have high optical transmittance and good resistance to photo degradation. As shown in Fig.3 (a)

is the prototype of the lens-walled compound parabolic concentrator for the CPV/D system: the length, height and width of it are 300.0 mm, 46.7 mm and 15.0 mm respectively. The whole CPV/D module consists of six lens-walled CPCs with the same structure. It should be noted that for the volume production of the concentrators, press modeling technology could be used, which will significantly reduce the system cost [18]. This issue will also be detailed discussed in the following section. The aluminum coating technology is used to process the reflection mirrors, and a reflectivity of around 85% could be achieved. To access the “daylighting window”, the outer reflector near the base area isn’t coated for sun rays to get through. The height of the non-coated area counting from the base is selected as 3 mm based on the structure optimization results [10]. For the actual engineering, multi-layer polymer film with high reflectivity which is non-corroding and non-conductive is recommended for a higher performance system.

3.1.2 Support structure design and construction

Due to the CNC machine precision, it’s hard to deal with the linkage area below the concentrator, which would also influence the optical property near the top part of the concentrator. Besides, considering that for the actual use, adopting the support structure could make the installation and later maintenance more convenient and easy. So six lens-walled CPCs are manufactured separately and then assembled together through the support structure (which has the same outer contour as the lens-walled CPC) as shown in Fig. 3 (b). The support structure for the experimental system is also manufactured through CNC wire cutting using PMMA. However, for the actual

application, it's better to use thick stainless steel reflector substrate, which is able to provide adequate structural rigidity for the concentrator and to conduct and dissipate heat, thus to reduce the solar cell temperature to enhance the concentrating PV performance.

3.1.3 PV absorber design

For the traditional concentrating PV device, the PV module can be laminated on a support plate without setting gaps, and making sure that the PV module is attached with the absorber area of the concentrator is enough. However for the CPV/D system, due to the introduction of the daylighting function, the gaps between each PV cell are required to allow sun rays to pass through as shown in Fig. 4. The support plate used in the experiment system is made by PMMA considering its simple machining process and high mechanical strength. Thus, the PV absorber contains two parts: a PMMA backing plate and mono-crystalline silicon solar cells. In order to transfer the heat away from the PV cells to the surroundings more efficiently thus to enhance the concentrating PV performance, the material such as aluminum is suggested to manufacture the back plate for the practical application.

3.1.4 Experimental box design

As shown in Fig. (d) is the experiment box, which is made by using the integrating sphere principle [29]. The photometric integrating box is a cubic box with its internal surface painted matt white (with the use of the nanometer high diffuse reflection material, YJ-NT made by China) therefore, the incoming sun rays can be diffusely reflected to the internal sensor, which was proposed by the UK Building

Research Establishment. The CPV/D window is installed on the top of the experiment box, and the other five surfaces of the experiment box all open a pore with the diameter of 50.0 mm for the installation of the digital illuminance meter to get the illuminance in it. The length, width and height of the experiment box is 360.0 mm, 385.5 mm and 450.0 mm respectively including the wall (which is 30.0 mm).

The detailed description about the key components of the experiment system and how they are assembled together are presented in Fig.3. As shown in Fig. 5 is the outdoor overall CPV/D experiment system. The experimental test rig is installed in the East-West orientation on the rooftop of Engineering Bldg. 2, University of Science and Technology of China, Anhui, Hefei, China (31.86°N, 117.28°E).

3.2 Experimental characterization of the CPV/D system (experimental procedure and test instruments description)

The PV cell used for the CPV/D system is the mono-crystalline-silicon PV cell as show in Fig. 4. In order to determine the working condition of the PV panel (main influence parameter is the temperature), three T-type thermocouples are attached to three different points on the back of the PV panel, and the positions of the thermocouples are also drawn in Fig.4.

Considering that the illuminance in the box may be different due to the sun motion, so during the entire test period, the illuminance is got from four facades of the experiment box. The detailed orientation of four facades for the east-west oriented

CPV/D window and test positions on each face are shown in Fig. 6. L_1 , L_2 , L_3 and L_4 represent four illuminometer positions.

The experimental characterization for the CPV/D system contains the concentrating PV performance and daylighting performance investigation. The (I-V) and (P-V) characteristics of the CPV/D system are derived by a portable solar module analyser (made by RS PRO[®], ISM-490, with an accuracy of $\pm 1\%$). The illuminance level in the experiment box is tested using the illuminometer (made by TES[®], with an accuracy of $\pm 3\%$). The temperature of the PV cell is measured using T-type thermocouples (with an accuracy of $\pm 0.2^\circ\text{C}$) named as T_1 , T_2 and T_3 which are distributed as shown in Fig. 4. The temperature in the experiment box is also measured by T-type thermocouples. Similarly, the ambient temperature is measured using a single thermocouple in a solar radiation shield to avoid the influence of radiation. Finally, the solar radiation on the front aperture of the CPV/D system is measured using a pyranometer (TBQ-2, with an accuracy of $\pm 2\%$). A portable data acquisition system (HIOKI, LR8401-21) are linked with the experimental test rig to automatically get the temperature and solar radiation data at a time interval of 10 s.

The experiment was conducted on 10th Aug. 2018. The weather condition on that day is sunny and windy, so sometimes there are some paper clouds in the sky but it flew away quickly. The electrical and illuminance data was collected every 20 minutes from 8:40 to 17:20. The main objective of the outdoor experiments focus on the actual daylighting and electrical performance of the CPV/D window, so the test

period is not continuous. During the test, the experiment system was exposed to the solar radiation but after the completion of a round of data collection, the whole system was covered to prevent the solar radiation. Every test last around 1-2 minutes.

4. Results and discussions

Instantaneous solar radiation on the plane of the CPV/D system on 10th Aug. is shown in Fig. 7. The weather condition on that day was very good except during noon time, when sometimes there were some paper clouds in the sky that weaken the solar radiation a little. Although the experiment is not continuous, the environment temperature is very high with very strong solar radiation, which may also make the temperature of the PV panel increase quickly. So the test conditions, such as temperature of the PV panel, solar radiation, environment temperature and wind speed during every round of testing are listed in Table 1. It should be noted that the temperature of the PV panel on three different test positions are close, the deviation between which are less than 1 °C, so the temperature of the PV panel given in table 1 is the average value of results from three test points (T_1, T_2, T_3).

4.1 The daylighting performance of the CPV/D system

The instantaneous illuminance in the box is shown in Fig. 8. As described above, the illuminance in the box is got from four facades. L_1, L_2, L_3 and L_4 represent the illuminance levels of the west, south, east and north façade respectively. From the results, it can be seen clearly that the illuminance level on different facades varies a little. The lowest value of the illuminance in the box is around 1000 lx during the

evening time while the highest value of that is around 9000 lx, which is pretty much corresponding with the actual inner situation of the buildings under the sunny weather condition (1000-5000lx on sunny day and 8000-12000lx at noon time). The changing tendency of the illuminance levels on four facades can be described as: in the morning, when the sun position in the sky is to the east, the illuminance value of the west wall is the highest while the east wall shows the lowest illuminance level; during the noon time when the sun position in the sky is near to the south-north vertical plane, the illuminance values of the south and north wall are a little higher than those of the east and west wall, and the illuminance level on the north wall is the strongest among four walls. Besides of that, the illuminance values of the east and west wall are very close; in the afternoon, when the sun position in the sky is to the west, the illuminance value of the east wall is highest than another three walls, and the difference value is very large between 15:40 and 16:40, while the illuminance levels on the other three walls are very close. It can be predicted that, as the time goes later than 17:20, the illuminance in the box would coverage to the same level as the decrease of the solar radiation. From the analysis, the main reason for the changing tendency of the illuminance level of four walls throughout the day is duo to the sun motion. On the one hand, in the morning, the sun rays hit the CPV/D window from the direction of east-to-west, so they are more likely to reach the east wall. Similarly, the sun rays path is from west to east so that they are more likely to reach the east wall in the afternoon. On the other hand, the shading effect near the frame structure should be noticed: In the morning, the east frame would cast a shadow on the neighboring area that would decrease the

illuminance value on the east façade as well, and the same situation will occur for the west façade in the afternoon. Therefore, the illuminance level on the west façade in the morning is highest while in the afternoon the highest values of the illuminance level appear on the east façade.

The inner view of the box throughout the day is shown in Fig. 9. The photos were taken during the test period through the pore on the north wall of the box and the photos at the whole points are selected to be displayed in the paper to reveal the actual daylighting performance of the CPV/D window. From the results, the inner environment of the box is illuminated well by the solar radiation and the brightness is very uniform. By the comparison of each photo, it's clearly that the brightness of the photo is different as the times changes, which means that the illuminance level in the box varies with time. From 9:00 to 13:00, the brightness in the box increases as the time goes by and it reaches the peak at around 13:00 then followed by a decreasing trend till to 17:00. It's obvious that the changing rule of the brightness in the box is consistent with the results shown in Fig. 8. On the sunny day during the summer, the illuminance level on the ground would exceed 100000 lx at noon. From the irradiation data presented in Fig. 7, the illuminance level on the front surface of the CPV/D window is in the range of 20400 to 114300 lx while the illuminance values in the integrating box only falls in the range of 923 to 9230 lx. From above analysis, the CPV/D window can obviously improve the illumination environment in a room in a day and effectively reduce the amount of light intensity entering the room to provide a

more uniform illumination condition. Even at noon time, it won't generate strong glare to make eyes uncomfortable, for the CPV/D window only allows a small portion of the solar radiation into the room for daylighting but captures most incoming solar radiation for the electricity generation, which would also reduce the heat gain of the building during the summer thus to save the air conditioning load.

4.2 The electrical performance of the CPV/D system

In the following section, the electrical performance of the CPV/D window on 10th of August will be detailedly presented. The I - V characteristics at various times are presented in Fig. 10 and Fig. 11 illustrates the variation of the power generation by the CPV/D window along with the voltage developed by it i.e. P - V characteristics. The two limiting parameters used to characterize the output of solar cells for given irradiance, operating temperature and area are [42]:

1. Short-circuit current (I_{sc}): the maximum current with the voltage of the solar cell at zero. And the short current of the non-concentrating solar cell is directly proportional to the total captured solar radiation;
2. Open-circuit current (V_{oc}): maximum voltage with the current of the solar cell at zero. The value of V_{oc} increases logarithmically with increased sunlight for the non-concentrating solar cell.

The short-circuit current of the CPV/D window on 10th Aug. is presented in Fig. 12. It should be noted that the short-circuit current of the solar cell increases with the temperature, due to the fact that the bandgap energy (E_g) decreases as the increase of the temperature and more photons have enough energy to create electron-hole pairs.

However, the effect of this is rather small. For silicon:

$$\frac{1}{I_{sc}} \frac{dI_{sc}}{dT} \approx +0.0006 \text{ } ^\circ\text{C}^{-1} \quad (4)$$

From the results displayed in Fig. 12, the change tendency of the short-circuit current produced by the CPV/D window throughout the day is similar with that of the solar radiation intensity. Different from the directly exposed solar cells, the use of the concentrator may influence the total solar radiation that reaches the PV cell due to different optical efficiency at different incidence angles. But from the results shown in Fig. 2, within the acceptance range of the concentrator, the optical efficiencies are very close. So the short-circuit current produced by the CPV/D window is also basically proportional to the solar irradiation intensity on the test day.

However, the PV module temperature has more obvious effect on its open-circuit voltage and *Fill Factor* (*FF*). For the silicon solar cells, the main effect of the increasing temperature is the reduction of the *Voc*, the *Fill Factor* and the hence the output. The temperature dependence of the *Voc* for silicon is determined by the following equations:

$$\frac{dV_{oc}}{dT} = \frac{[V_{g0} - V_{oc} + \gamma(kT/q)]}{T} \approx -2mV^\circ\text{C}^{-1} \quad (5)$$

$$\frac{1}{V_{oc}} \frac{dV_{oc}}{dT} \approx -0.003^\circ\text{C}^{-1} \quad (6)$$

The open-circuit voltage (*Voc*) on the test day is show in Fig. 13. From the results, it's obvious that the open-circuit voltage during the all-day test period keeps at almost the same level with only small difference value due to the temperature of the PV panel didn't reach very high value during noon time. However, the *Voc* of the CPV/D

window at noon time when the solar radiation is strongest still shows a small decreasing trend with the increase of the solar module temperature.

The *Fill Factor (FF)* of a PV module is defined as:

$$FF = \frac{P_m}{V_{oc} I_{sc}} \quad (7)$$

Which can also be calculated by the use of the normalized V_{oc} as follows:

$$FF \approx \frac{v_{oc} - \ln(v_{oc} + 0.72)}{v_{oc} + 1} \quad (8)$$

Where v_{oc} is defined as the “normalized V_{oc} ”, which is calculated by [43]:

$$v_{oc} = V_{oc} \cdot \frac{q}{n \cdot k \cdot T} \quad (9)$$

k --Boltzmann constant = $1.38 \times 10^{-23} \text{ J/K}$, q —charge of electron = 1.6×10^{-19} , and n —diode ideality factor = 1.45 .

The *FF* values during the test period present a fluctuant changing tendency (Fig. 14). This trend was mainly affected by the changing of the PV panel temperature and the non-uniform solar radiation that falls on the PV module and the effect of the non-uniform illumination might be a more obvious one [44, 45]. Obviously, the nearer the *Fill Factor* is to unity, the higher the quality of the cell especially for the concentrating PV devices [46, 47]. For the CPV/D window, during the all-day test when the highest temperature of the concentrating PV module exceeds 50°C, the average value of *FF* can still remain at 75.2%, this is due to the relative more uniform flux distribution that falls on the PV cell compared with other kinds of the miniature low-concentration ratio concentrators. For the further optimization, those impacts can be reduced by improving the uniformity of the solar radiation that falls on the PV

panel and adopting active cooling technology. However, the latter strategy should better consider the application of CPV/T/D for the buildings and actual enforcement mode.

The maximum power output (P_m) of the CPV/D window is shown in Fig. 15. The changing tendency throughout the day is similar with that of the short-circuit current. The power output of the CPV/D window is 2500 mW at 11:40 when the solar radiation intensity is 1041 Wm^{-2} . As described above, during noon time, sometimes there are some paper cloudy in the sky, which makes the experiment results fluctuant. But it's clearly that P_m is still larger than 2100 mW, for the solar intensity is still very strong even though the paper clouds block some solar radiation. Besides of the regular factor that may influence of the maximum power of the flat PV module such as temperature solar radiation intensity, P_m of the concentrating PV device is also affected by the flux distribution on the receiver and optical efficiency of the concentrator [30].

4.3 *The temperature in the experimental box.*

The temperature variation of the environment and top/medium/bottom area in the box is shown in Fig. 16. From the results, the temperature in the box presents an increasing trend throughout the day. The temperature of the bottom area in the box is highest while that of medium is lowest. This is mainly due to the position of the test points: the thermocouple to test the temperature of the top area is close to the PV module, so the near space is heated by the PV module for the reason that even after a

short time of exposure to the solar radiation, the PV cell temperature increases very quickly. For the bottom area, during noon time, when sun rays strike the CPV/D window close to the normal incidence angles, the escape sun rays for the daylighting reaches the floor of the box, which makes the temperature of floor increases thus heat the nearby space. During noon time, the bottom area temperature shows fluctuant change tendency which is the same as that of the solar radiation intensity during noon time, which further approves the analysis above. From the overall comparison, due to the fact that the test is not continuous, the temperature in the box didn't reach very high values, which is only a little larger than the environment temperature. So the CPV/D window can to some extent solve the overheating and dazzling problem of the interior environment during the summer when the solar radiation is very strong as compared with the glass roof, for the reason that CPV/D window only allows a small portion of solar radiation into the room for daylighting. The results may be different for the continuous test and this inspires the application of the CPV/T/D system for the buildings with a better system arrangement form: the increase of the temperature in the experiment box shows the potential of building heating in the winter thus to achieve a higher usage ratio of the solar energy, namely through concentrating photovoltaic/thermal/daylighting system.

4.4 Cost assessment of the concentrator for the CPV/D system

Compared with the traditional PV module, the biggest difference is the introduction of the concentrator. Considering that PV cell has a mature commercial market, thus in this section, the cost assessment of the concentrator for the CPV/D

system has been conducted.

For the volume production of the CPV/D window, the gravity die casting technology will be used to manufacture the concentrator. Although the injection mould costs a lot of money (maybe no less than \$ 30k), a mould is able to make millions of concentrators, which reflects that cost impact due to the mould per unit concentrator is significantly less, thus the cost of the mould is not included [48]. Feng et al. estimated that for the dielectric CPC, the cost of the PMMA is $110 \text{ \$ m}^{-2}$ [31] and the material used for the lens-walled CPC is only $1/4$ — $1/3$ to that of the dielectric CPC. The material cost of the CPV/D window is list in Table 2. The total manufacturing price value of the CPV/D window is high for the small systems manufactured ($290.25 \text{ \$ m}^{-2}$), and a reduction of up to 46.5% to $155.17 \text{ \$ m}^{-2}$ could be expected in volume production. Recently, the price of the roof made by the glass curtain wall is about 160 – $320 \text{ \$ m}^{-2}$ [29]. It's clearly that the cost of the CPV/D window is in the price range of the traditional glass roof, which means that CPV/D window is better than the glass roof.

5 Conclusions

This paper displays a novel CPV/D window for the substitution of the traditional building skylight for green building roof. This novel design combines both the renewable electricity generation and daylighting for the multi-function window to be used on the buildings. It could achieve a higher usage ratio of the solar energy in the modern architecture with the new CPV/D window. And through the ray-tracing

simulation results, at lower incidence angles (namely within the acceptance range of the lens-walled CPC), the transmittance of the CPV/D window remains at almost the same level which is around 10%. But when the incidence angle exceeds the acceptance range, the transmittance of the CPV/D window reaches very high value (almost 80%).

The prototype of the concentrating photovoltaic/daylighting window has been designed, constructed and experimentally characterized. From the experiment results, the highest value of the illumination is around 9000lx while the lowest value is around 1000 lx with the outside illuminance level exceeds 100000lx during noon time, which indicates that the concentrating photovoltaic/daylighting window can improve the visual comfort for the building interior environment and it can also avoid the building interior environment from overheating and dazzling at noon compared with the transparent window thus to reduce the air conditioning load. It's also found that the sun motion has an obvious effect on the illumination distribution in the experiment box, and the effect is dual: the direction of the sun rays path and the shadow casted by the frame. The maximum power produced by the CPV/D window is 2500 mW at noon time. Due to the relative uniform flux distribution that falls on the PV cell, the average value of the FF can still be 75.5% in a day despite the increase in the PV module temperature.

Through the preliminary economic analysis, the total manufacturing price value of the CPV/D window is high for the small systems manufactured ($290.25 \text{ \$ m}^{-2}$), and a reduction of up to 46.5% to $155.17 \text{ \$ m}^{-2}$ could be expected in volume production.

As predicted, it's clearly that the cost of the CPV/D window is in the price range of the traditional glass roof, which means that CPV/D window is better than the glass roof. Due to the fact that only a small portion of incoming solar radiation is transferred into the electricity while the most of it is dissipated as heat, thus in order to achieve a higher-efficiency system, it's better to use the thermal energy for the building heating in the winter as the concentrating photovoltaic/thermal/daylighting (CPV/T/D) system. The detailed system design, experimental study and numerical prediction work about this issue will be conducted in the future.

Acknowledgement:

The study was sponsored by the Project of EU Marie Curie International Incoming Fellowships Program (745614), the National Natural Science Foundation of China (NSFC 51476159, 51776193, and 5171101721), International Technology Cooperation Program of the Anhui Province of China (BJ2090130038), and Fundamental Research Funds for the Central Universities (WK6030000099). The authors would like to thank Prof. Zheng Hongfei (School of Mechanical Engineering, Beijing Institute of Technology, China) for his assistance in the software simulation.

References:

- [1] Omer AM. Energy, environment and sustainable development. *Renewable and Sustainable Energy Reviews*, 2008; 12: 2265-2300.
- [2] EIA (US Energy Information Administration). Independent statistics and analysis: how much electricity is used for lighting in the United States; 2017.
- [3] Meng Tian, Li Zhang, Yuehong Su, Qingdong Xuan, Guiqiang Li, Hui Lv. An evaluation study of miniature dielectric crossed compound parabolic concentrator (dCCPC) panel as skylights in building energy simulation. *Solar Energy* 2019; 179: 264-278.
- [4] Zheng Hongfei. Experimental study on an enhanced falling film evaporation–air flow absorption and closed circulation solar still. *Energy* 2001; 26: 401-412.
- [5] Chow TT, He W and Ji J. An experimental study of façade-integrated photovoltaic/water-heating system *Applied Thermal Engineering* 2007; 27: 37-45.
- [6] Muhammad-Sukki F, Abu-Bakar SH, Ramirez-Iniguez R, McMeekin SG, Stewart BG and Sarmah N. Mirror symmetrical dielectric totally internally reflecting concentrator for building integrated photovoltaic systems. *Applied Energy* 2014; 113: 32-40.
- [7] International Energy Agency (IEA). Potential for building integrated photovoltaics. Report IEA-PVPS T7-4: 2002 (Summary), IEA.
- [8] Oliver M and Jackson T. Energy and economic evaluation of building-integrated photovoltaics *Energy* 2001; 26: 431-439.
- [9] Singh GK. Solar power generation by PV (photovoltaic) technology: A review.

- Energy 2013; 53: 1-13.
- [10] Li G, Xuan Q, Pei G, Su Y, Lu Y, Ji J. Life-cycle assessment of a low-concentration PV module for building south wall integration in China. *Applied Energy* 2018; 215: 174-185.
- [11] Chong K, Onubogu NO, Yew T, Wong C, Tan W. Design and construction of active daylighting system using two-stage non-imaging solar concentrator. *Applied Energy* 2017; 207: 45-60.
- [12] Xu Q, Ji Y, Riggs B, Ollanik A, Farrar-Foley N, Ermer JH, et al. A transmissive, spectrum-splitting concentrating photovoltaic module for hybrid photovoltaic-solar thermal energy conversion. *Solar Energy* 2016; 137: 585-593.
- [13] Abu-Bakar SH, Muhammad-Sukki F, Freier D, Ramirez-Iniguez R, Mallick TK, Munir AB, et al. Performance analysis of a novel rotationally asymmetrical compound parabolic concentrator. *Applied Energy* 2015; 154: 221-231.
- [14] Wang Q, Zhu Z, Wu G, Zhang X, Zheng H. Energy analysis and experimental verification of a solar freshwater self-produced ecological film floating on the sea. *Applied Energy* 2018; 224: 510-526.
- [15] Winston R. Principles of solar concentrators of a novel design. *Solar Energy* 1974; 16: 89-95.
- [16] Rabl A, Gallagher OO, Winston R. Design and Test of Non-Evacuated Solar Collectors with Compound Parabolic Concentrators, University of Chicago.
- [17] Renno C, Petito F. Design and modeling of a concentrating photovoltaic thermal (CPV/T) system for a domestic application. *Energy and Buildings* 2013;

2:392-402.

- [18] Mallick TK, Eames PC, Hyde TJ, Norton B. The design and experimental characterisation of an asymmetric compound parabolic photovoltaic concentrator for building facade integration in the UK. *Solar Energy* 2004; 77: 319-327.
- [19] Mallick TK, Eames PC, Norton B. Non-concentrating and asymmetric compound parabolic concentrating building facade integrated photovoltaics: An experimental comparison. *Solar Energy* 2006; 80: 834-849.
- [20] Lu W, Wu Y, Eames P. Design and development of a Building Façade Integrated Asymmetric Compound Parabolic Photovoltaic concentrator (BFI-ACP-PV). *Applied Energy* 2018; 220: 325-336.
- [21] Su Y, Riffat SB, Pei G. Comparative study on annual solar energy collection of a novel lens-walled compound parabolic concentrator (lens-walled CPC). *Sustainable Cities and Society* 2012; 4: 35-40.
- [22] Li G, Pei G, Ji J, Su Y, Zhou H, Cai J. Structure optimization and annual performance analysis of the lens-walled compound parabolic concentrator. *International Journal of Green Energy* 2016; 13: 944-950.
- [23] Guiqiang L, Gang P, Yuehong S, Jie J, Riffat SB. Experiment and simulation study on the flux distribution of lens-walled compound parabolic concentrator compared with mirror compound parabolic concentrator. *Energy* 2013; 58: 398-403.
- [24] Guiqiang L, Gang P, Yuehong S, Yunyun W, Jie J. Design and investigation of a novel lens-walled compound parabolic concentrator with air gap. *Applied*

- Energy 2014; 125: 21-27.
- [25] Li G, Pei G, Yang M, Ji J, Su Y. Optical evaluation of a novel static incorporated compound parabolic concentrator with photovoltaic/thermal system and preliminary experiment. *Energy Conversion and Management* 2014; 85: 204-211.
- [26] Li G, Pei G, Ji J, Yang M, Su Y, Xu N. Numerical and experimental study on a PV/T system with static miniature solar concentrator. *Solar Energy* 2015; 120: 565-574.
- [27] Li G, Pei G, Ji J, Su Y. Outdoor overall performance of a novel air-gap-lens-walled compound parabolic concentrator (ALCPC) incorporated with photovoltaic/thermal system. *Applied Energy* 2015; 144: 214-223.
- [28] Xuan Q, Li G, Pei G, Ji J, Su Y, Zhao B. Optimization design and performance analysis of a novel asymmetric compound parabolic concentrator with rotation angle for building application. *Solar Energy* 2017; 158: 808-818.
- [29] Xuan Q, Li G, Pei G, Su Y, Ji J. Design and Optical Evaluation of a Novel Asymmetric Lens-Walled Compound Parabolic Concentrator (ALCPC) Integration with Building South Wall. *Journal of Daylighting* 2017; 4: 26-36.
- [30] Li G, Xuan Q, Lu Y, Pei G, Su Y, Ji J. Numerical and lab experiment study of a novel concentrating PV with uniform flux distribution. *Solar Energy Materials and Solar Cells* 2018; 179: 1-9.
- [31] Feng C, Zheng H, Wang R, Yu X, Su Y. A novel solar multifunctional PV/T/D system for green building roofs. *Energy Conversion and Management* 2015; 93:

63-71.

- [32] Xu Yu, Yuehong Su, Hongfei Zheng, Saffa Riffat. A study on use of miniature dielectric compound parabolic concentrator (dCPC) for daylighting control application. *Building and Environment* 2014; 74: 75-85.
- [33] Meng Tian, Xu Yu, Yuehong Su, Hongfei Zheng, Saffa Riffat. A study on incorporation of transpired solar collector in a novel multifunctional PV/Thermal/Daylighting (PV/T/D) panel. *Solar Energy* 2018; 165: 90-99.
- [34] K Shanks, Hasan Baig and Ashley Knowles, et al. The Assembly of Embedded Systems for Integrated Photovoltaic windows in Rural Buildings (E-IPB). The 9th edition of the international SOLARIS conference.
- [35] Li G, Xuan Q, Zhao X, Pei G, Ji J, Su Y. A novel concentrating photovoltaic/daylighting control system: Optical simulation and preliminary experimental analysis. *Applied Energy* 2018; 228: 1362-1372.
- [36] Ilami N, Mallick TK, Mc Neil DA. Optical characterisation of 3-D static solar concentrator. *Energy Conversion and Management* 2012; 64: 579-586.
- [37] Saleh Ali IM, O Donovan TS, Reddy KS, Mallick TK. An optical analysis of a static 3-D solar concentrator. *Solar Energy* 2013; 88: 57-70.
- [38] Muhammad-Sukki F, Abu-Bakar SH, Ramirez-Iniguez R, McMeekin SG, Stewart BG, Sarmah N, et al. Mirror symmetrical dielectric totally internally reflecting concentrator for building integrated photovoltaic systems. *Applied Energy* 2014; 113: 32-40.
- [39] Chemisana D, Ibáñez M, Barrau J. Comparison of Fresnel concentrators for

- building integrated photovoltaics. *Energy Conversion and Management* 2009; 50: 1079-1084.
- [40] Zheng H, Tao T, Dai J, Kang H. Light tracing analysis of a new kind of trough solar concentrator. *Energy Conversion and Management* 2011; 52: 2373-2377.
- [41] Y. Su, G. Pei, S. B. Riffat, and H. Huang, A novel lens-walled compound parabolic concentrator for photovoltaic applications. *Journal of Solar Energy Engineering*, 134 (2012) 021010.
- [42] Shockley, W. & Queisser, H.J. Detailed balance limit of efficiency of p-n junction solar cells. *Journal of Applied Physics* 1961; 32: 510 - 519.
- [43] Green, M.A. Accuracy of analytical expressions for solar cell fill factors. *Solar Cells* 1982; 7: 337 - 340.
- [44] Luque A, Sala G, Arboiro JC. Electric and thermal model for non-uniformly illuminated concentration cells. *Solar Energy Materials and Solar Cells* 1998; 51: 269-90.
- [45] Stacey RW, McCormick PG. Effect of concentration on the performance of flat plate photovoltaic modules. *Solar Energy* 1984; 33(6): 565-9.
- [46] Guiqiang Li, Qingdong Xuan, Gang Pei, Yuehong Su, Jie Ji. Effect of non-uniform illumination and temperature distribution on concentrating solar cell - A review. *Energy* 2018; 144: 1119-1136.
- [47] Li Guiqiang, Pei Gang, Su Yuehong, Ji Jie, Saffa B. Riffat. Experiment and simulation study on the flux distribution of lens-walled compound parabolic concentrator compared with mirror compound parabolic concentrator. *Energy*

2013; 58: 398-403.

- [48] Mallick T, Eames P. Design and fabrication of low concentrating second generation PRIDE concentrator. *Solar Energy Materials and Solar Cells* 2007; 91: 597-608.

ACCEPTED MANUSCRIPT

Figure captions:

Fig. 1. (a) The structure of the concentrator of the CPV/D module; (b) the prototype of the concentrator.

Fig.2. The simulation and experiment optical efficiency and daylighting efficiency of the CPV/D module at different incidence angles.

Fig. 3. The picture of the CPV/D system and experiment box: (a) concentrator; (b) support structure in which the concentrators are put; (c) CPV/D module; (d) experiment box for the experiment; (e) overall diagram of the CPV/D experiment system.

Fig.4. The PV module used in the experiment and the temperature test points for the PV panel (T1, T2, T3 represent thermocouples)

Fig. 5. The picture of the overall outdoor experiment system.

Fig. 6. The orientation of four facades of the experiment box and the points for the illumination test in the box (L_1 , L_2 , L_3 , L_4 represent four illuminometer positions).

Fig.7. Instantaneous solar radiation on the plane of the CPV/D system on 10th Aug.

Fig. 8. Illumination in the box.

Fig. 9. Inner view of the box during the all-day test. (The photos were taken from the L_4 pore on the north facade).

Fig. 10. I-V curves at different times of a day.

Fig. 11. P-V curves at different times of a day.

Fig. 12. Short-circuit current of the CPV/D module.

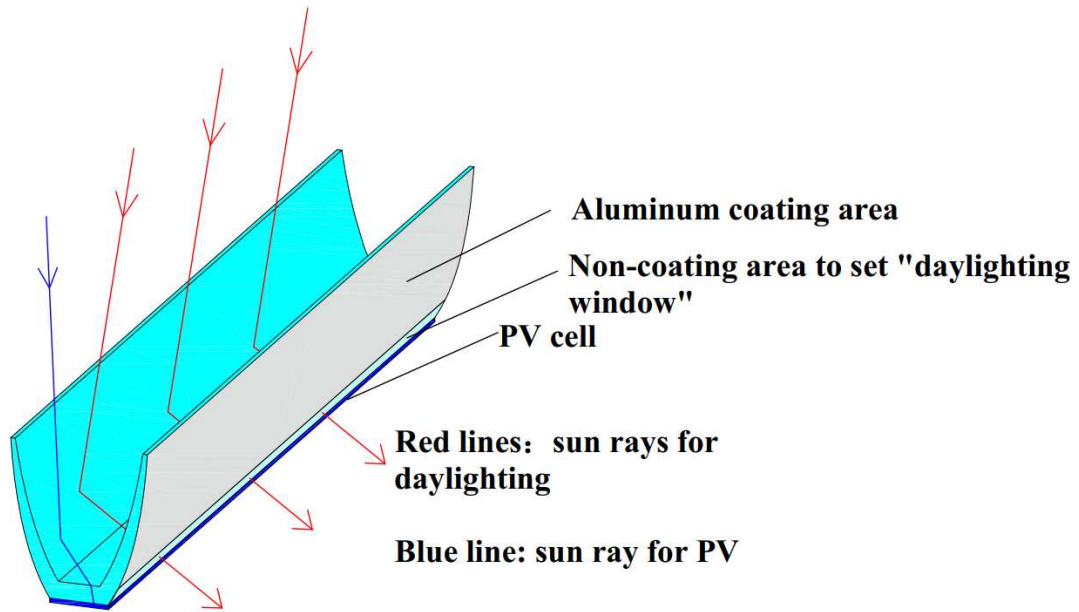
Fig. 13. Open-circuit voltage of the CPV/D module.

Fig. 14. *Fill Factor* of the CPV/D module.

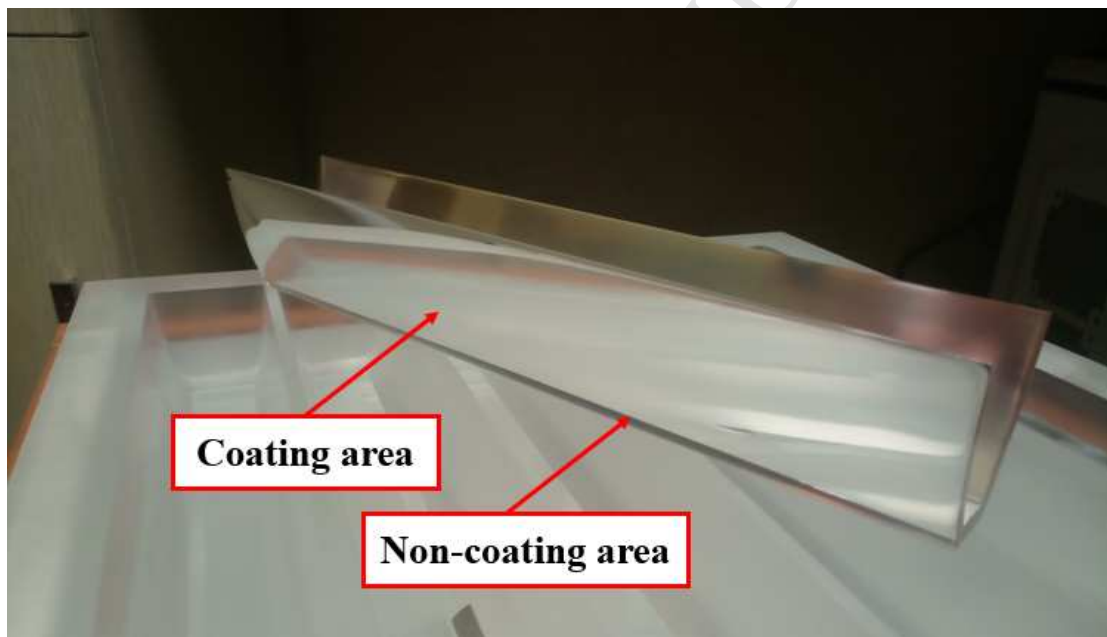
Fig. 15. Maximum power of the CPV/D module.

Fig. 16. The temperature of the environment and top\medium\bottom area in the box.

ACCEPTED MANUSCRIPT



(a)



(b)

Fig. 1. (a) The structure of the concentrator of the CPV/D module; (b) the prototype of the concentrator.

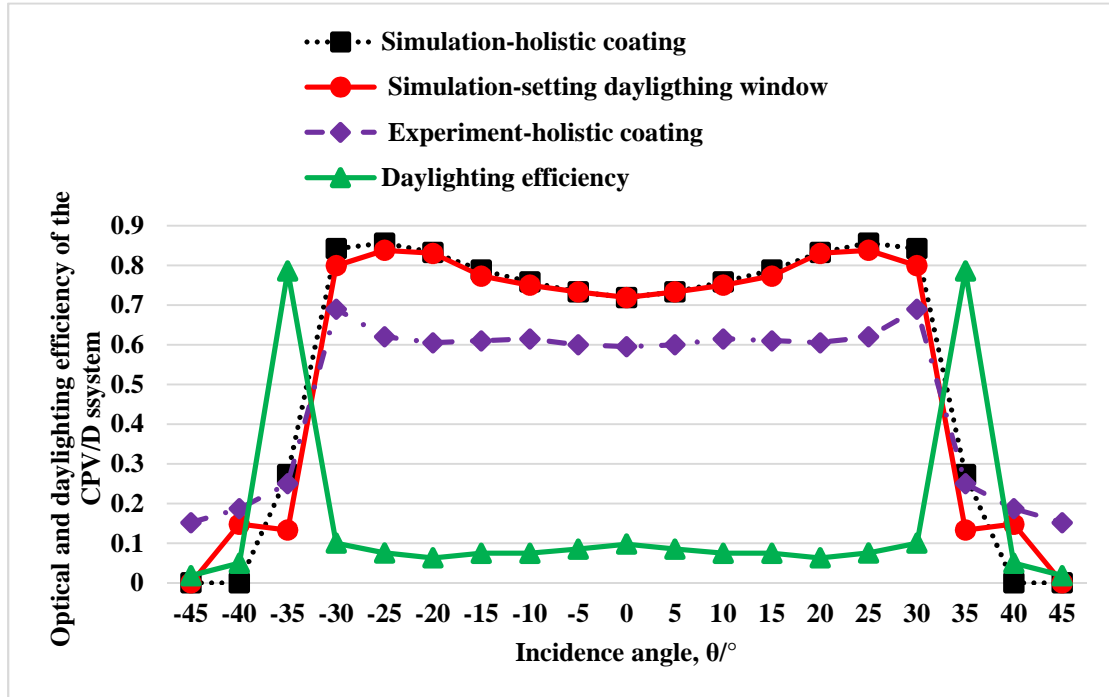


Fig.2. The simulation and experiment optical efficiency and daylighting efficiency of the CPV/D module at different incidence angles.

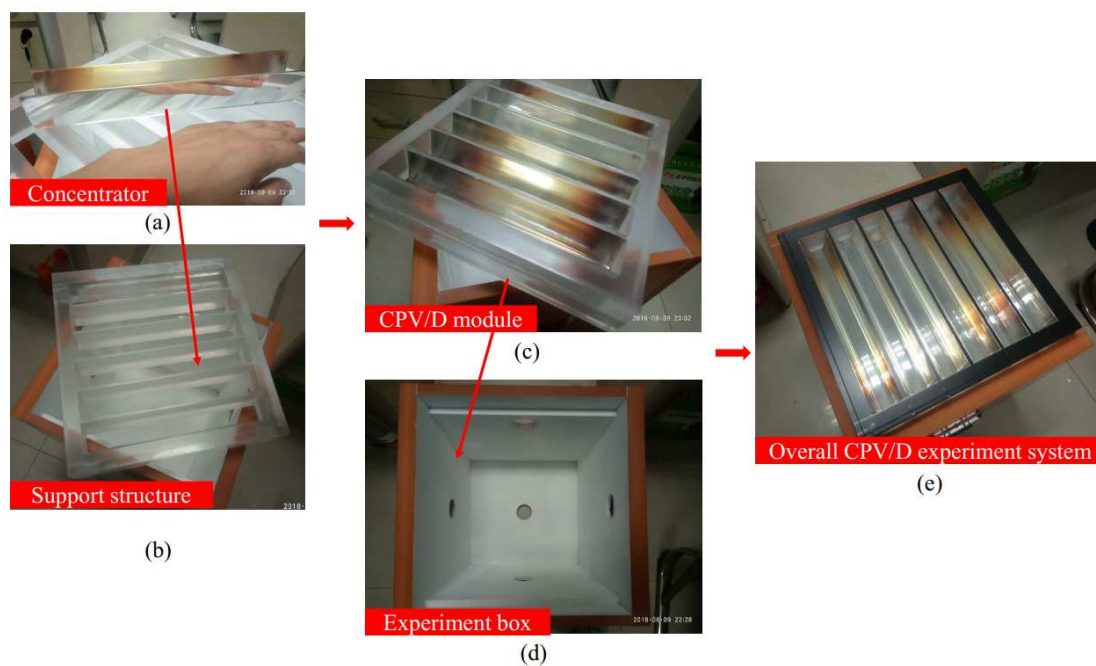


Fig. 3. The picture of the CPV/D system and experiment box: (a) concentrator; (b) support structure in which the concentrators are put; (c) CPV/D module; (d) experiment box for the experiment; (e) overall diagram of the CPV/D experiment system.

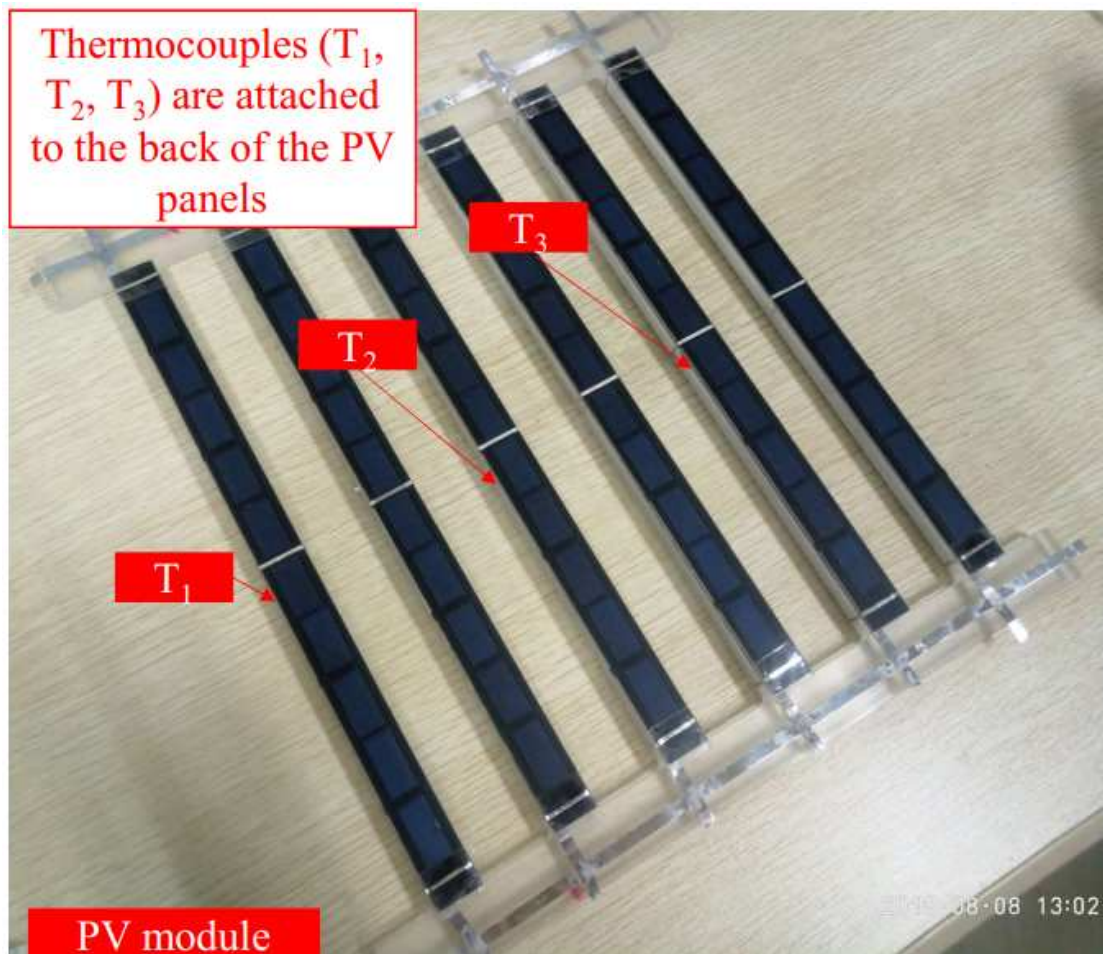


Fig.4. The PV module used in the experiment and the temperature test points for the PV panel (T_1 , T_2 , T_3 represent thermocouples).

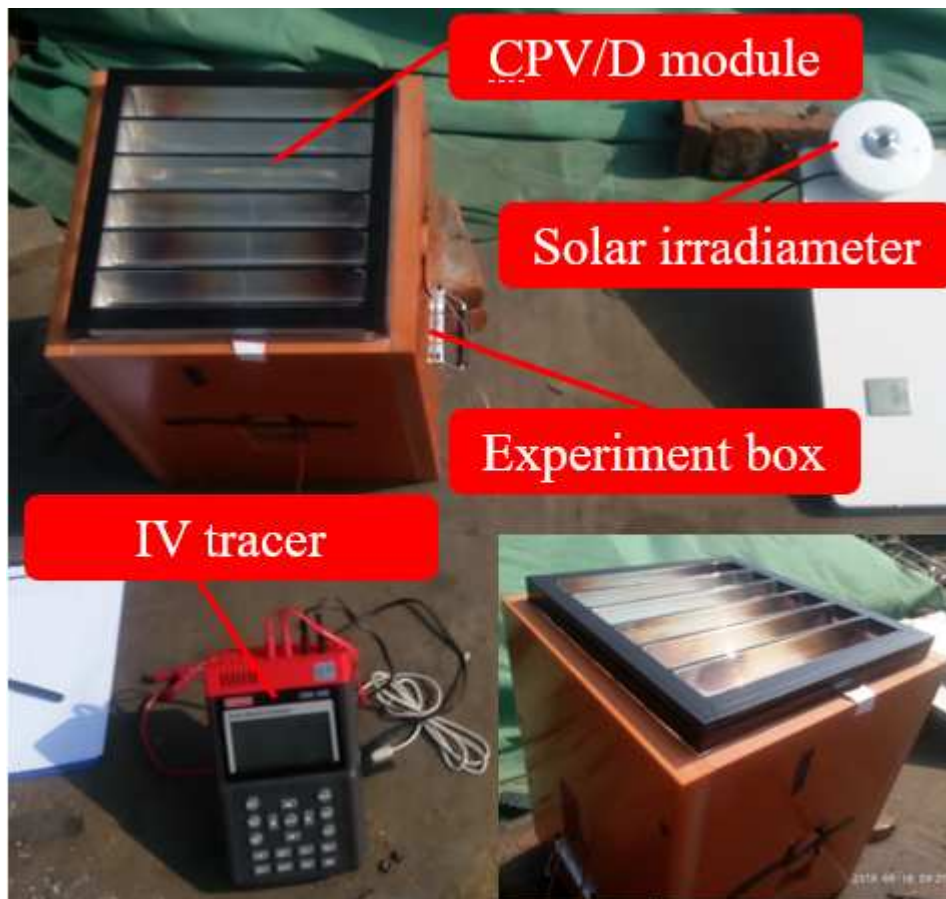


Fig. 5. The picture of the overall outdoor experiment system.

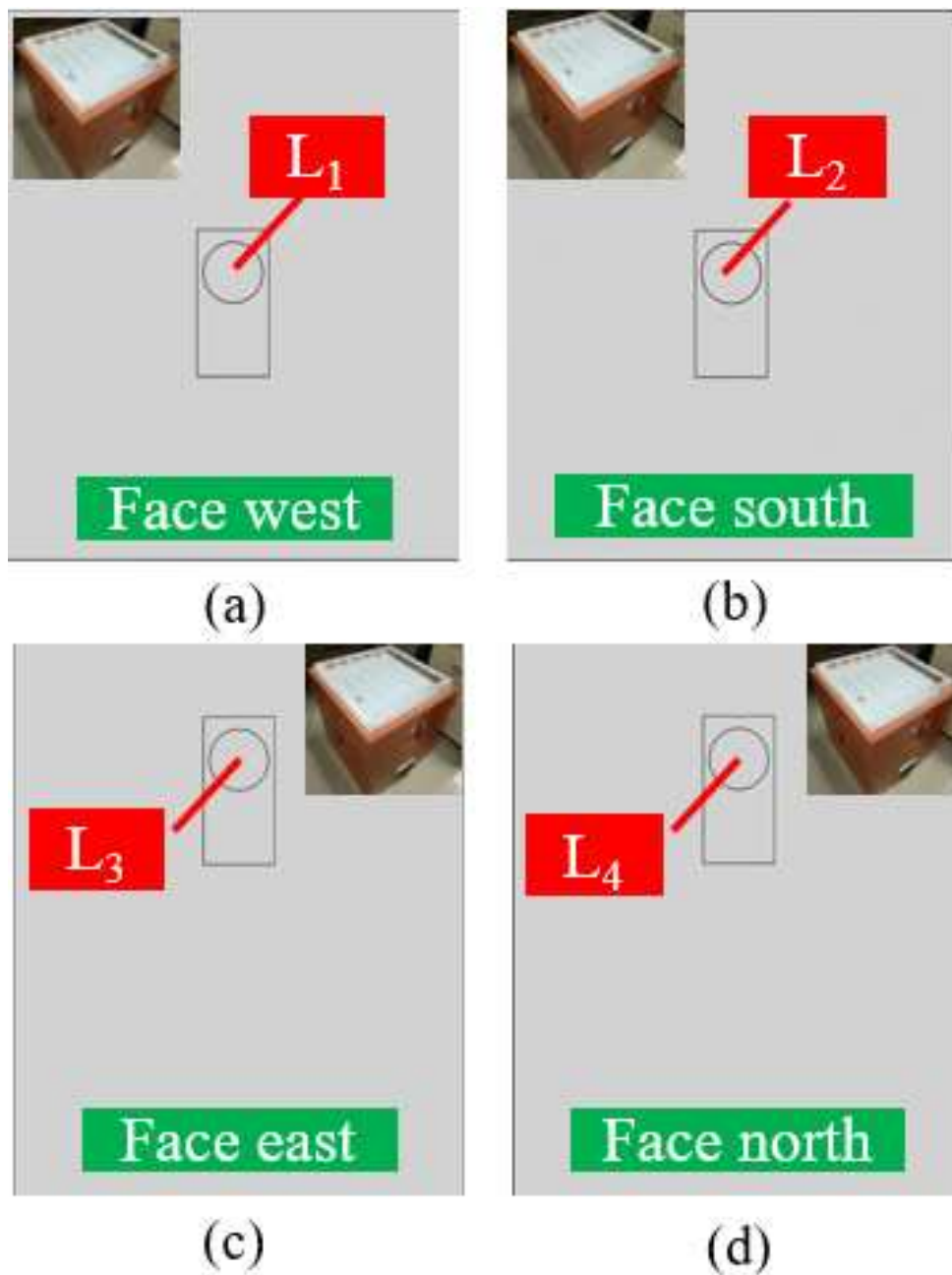


Fig. 6. The orientation of four facades of the experiment box and the points for the illumination test in the box (L_1 , L_2 , L_3 , L_4 represent four illuminometer positions).

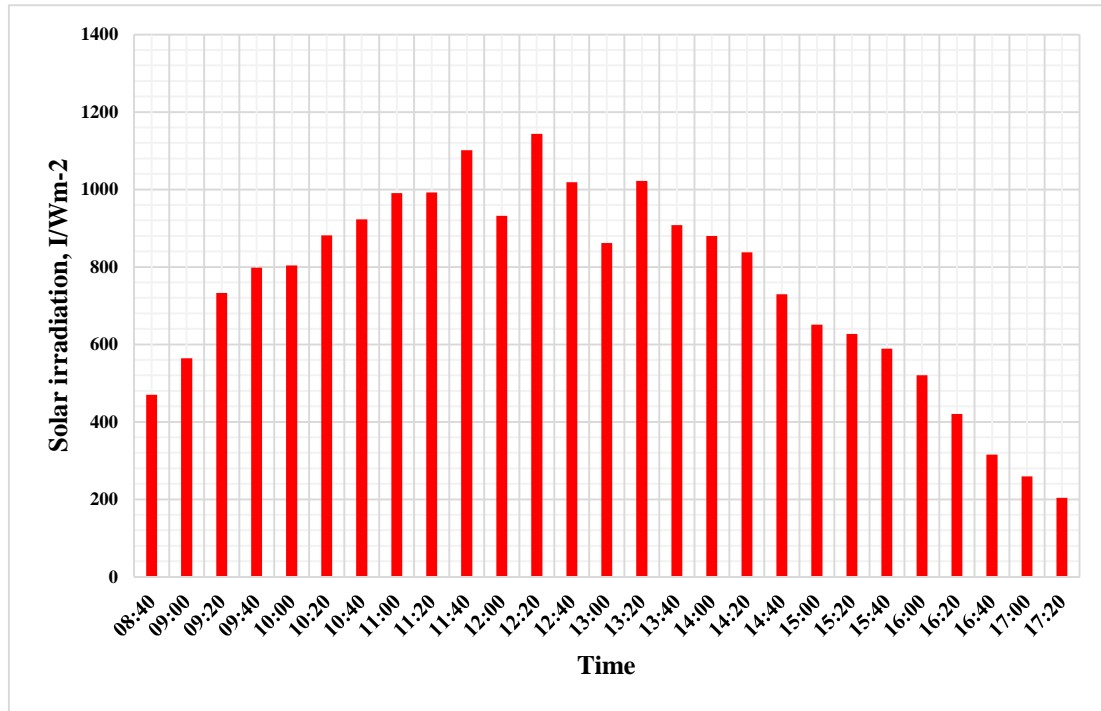


Fig.7. Instantaneous solar radiation on the plane of the CPV/D system on 10th Aug.

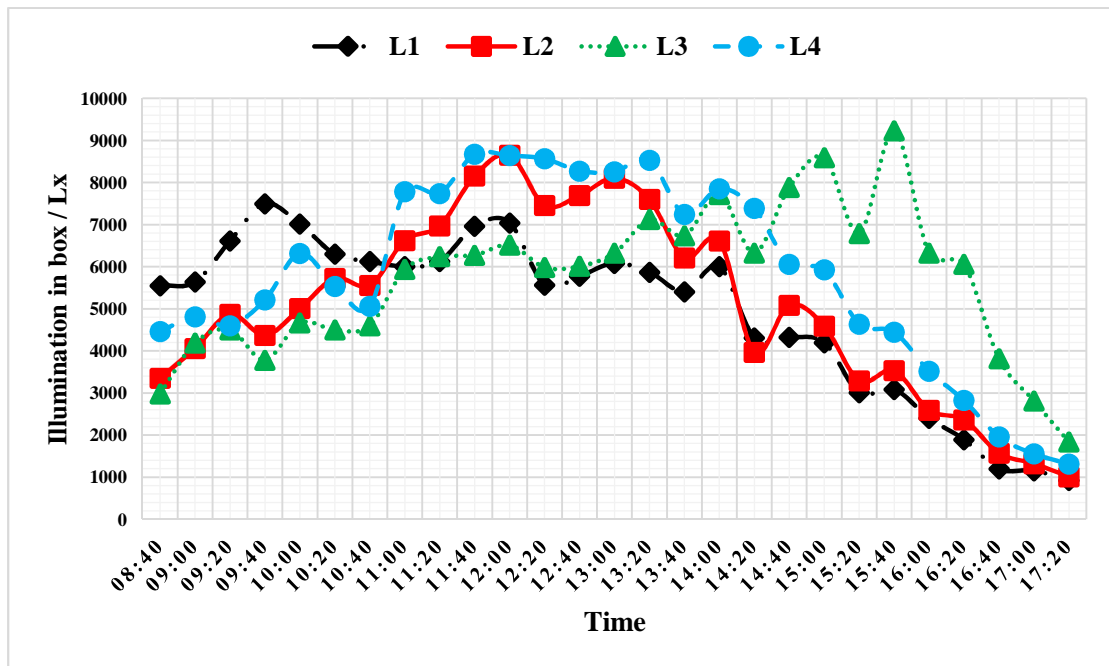
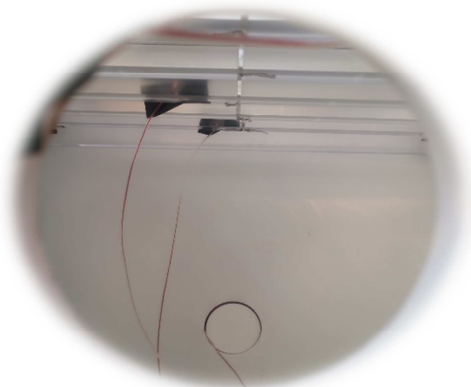


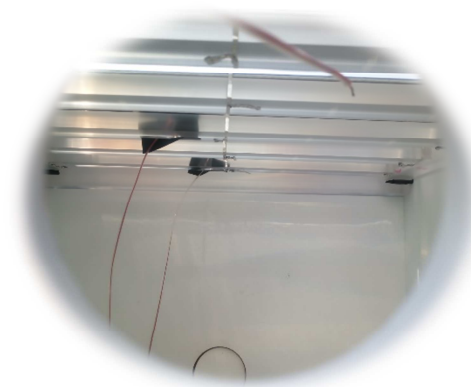
Fig. 8. Illumination in the box.



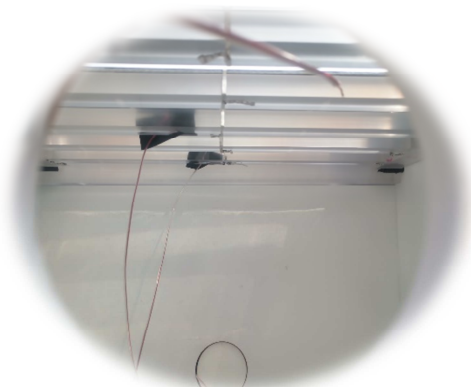
9:00



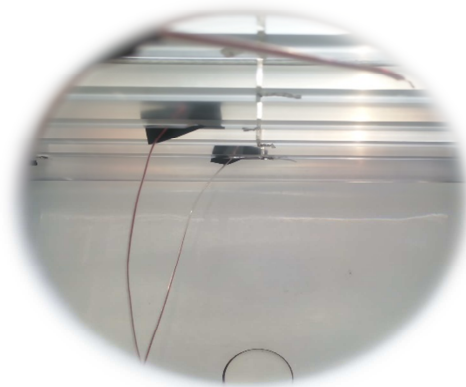
10:00



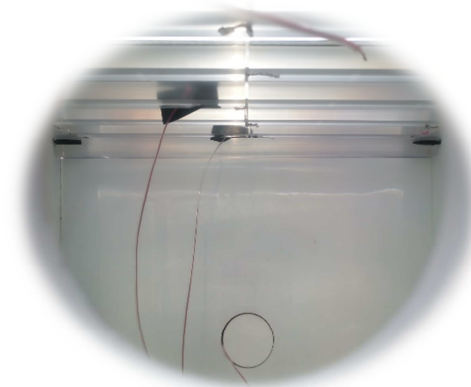
11:00



12:00



13:00



14:00

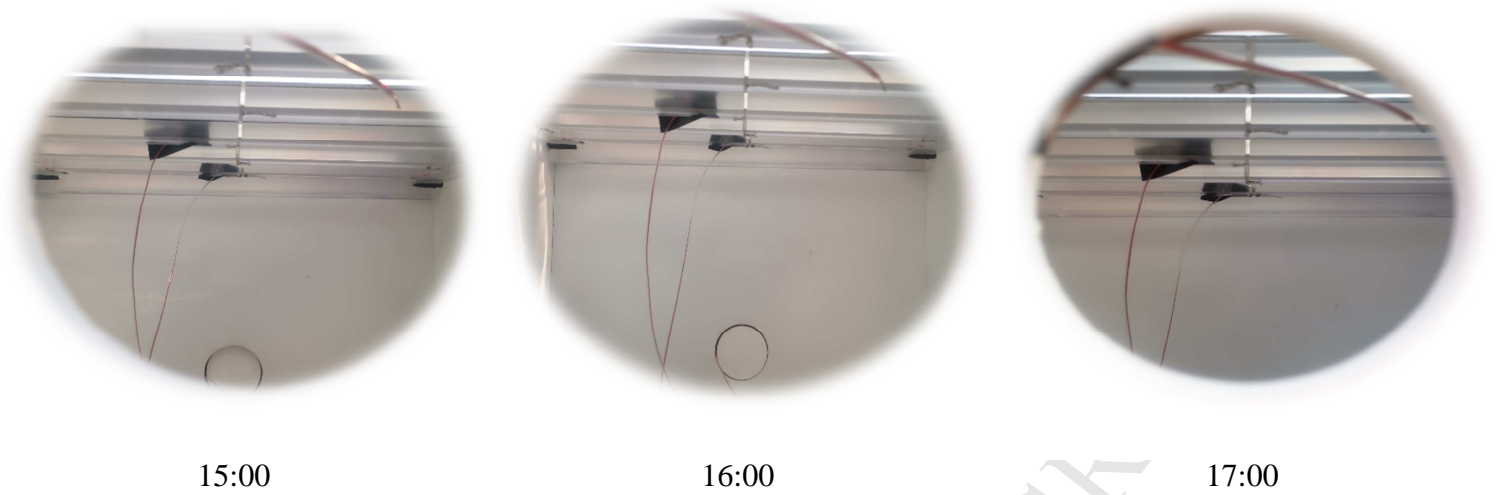


Fig. 9. Inner view of the box during the all-day test. (The photos were taken from the L₄ pore on the north facade).

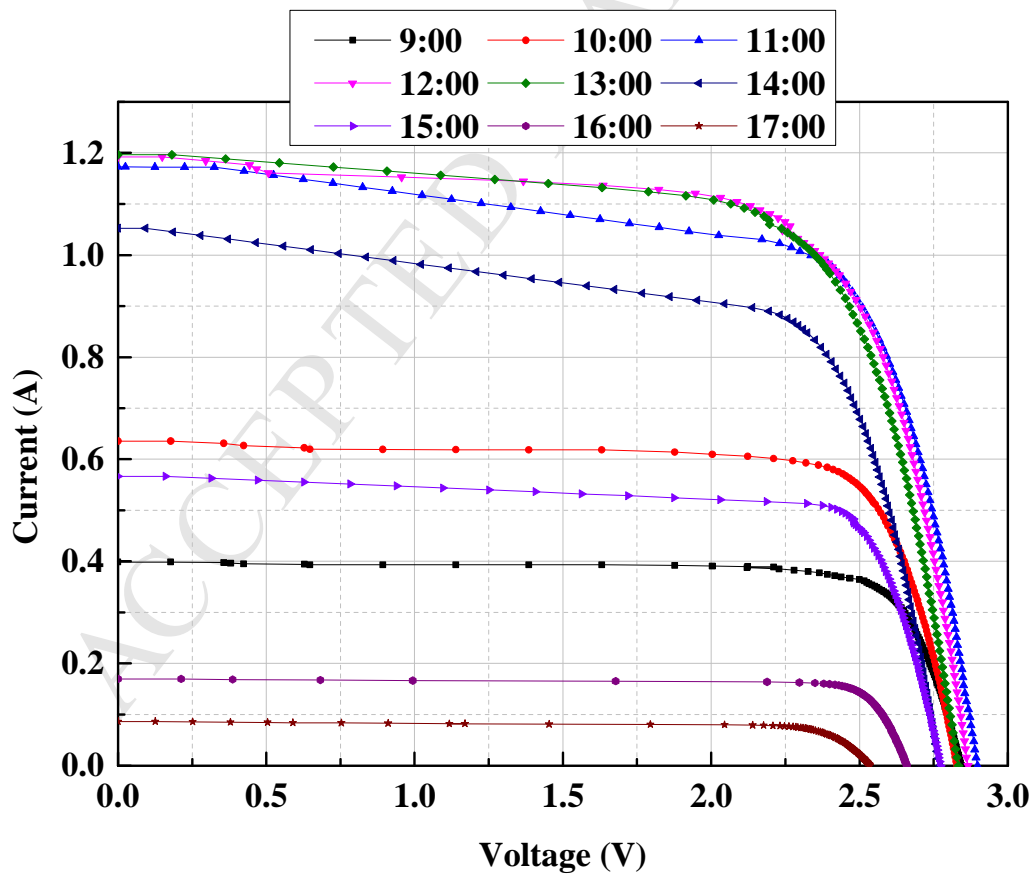


Fig. 10. I-V curves at different times of a day.

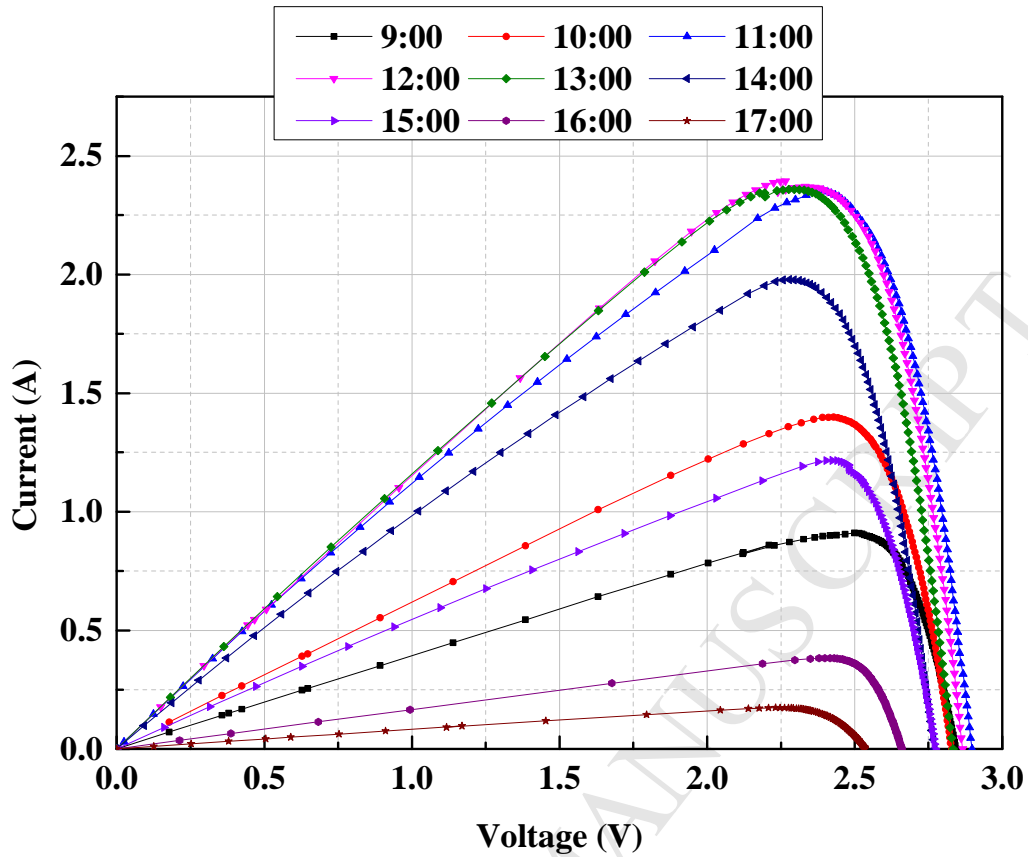


Fig. 11. P-V curves at different times of a day.

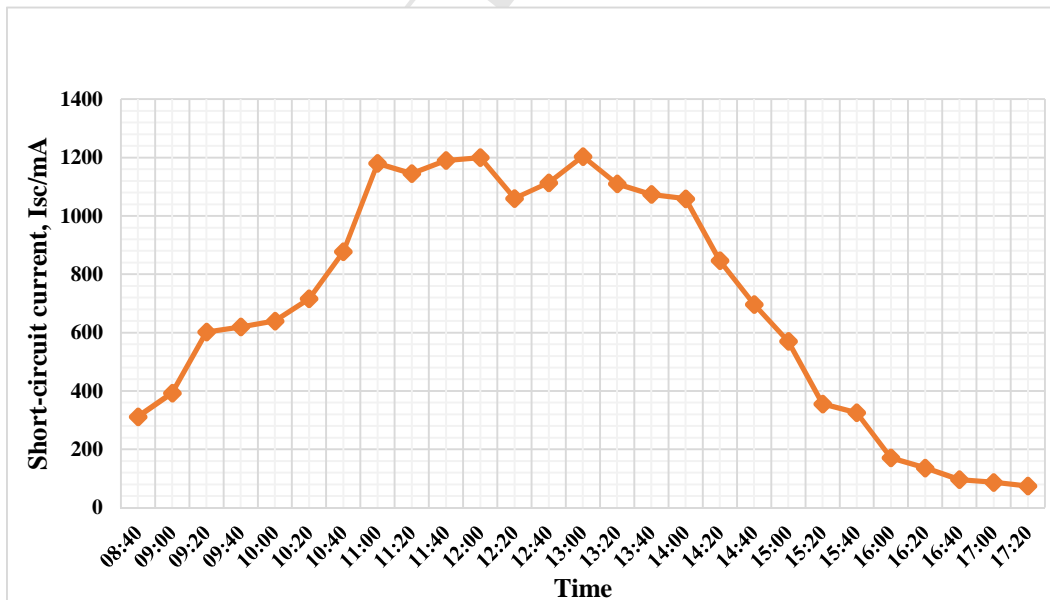


Fig. 12. Short-circuit current of the CPV/D module.

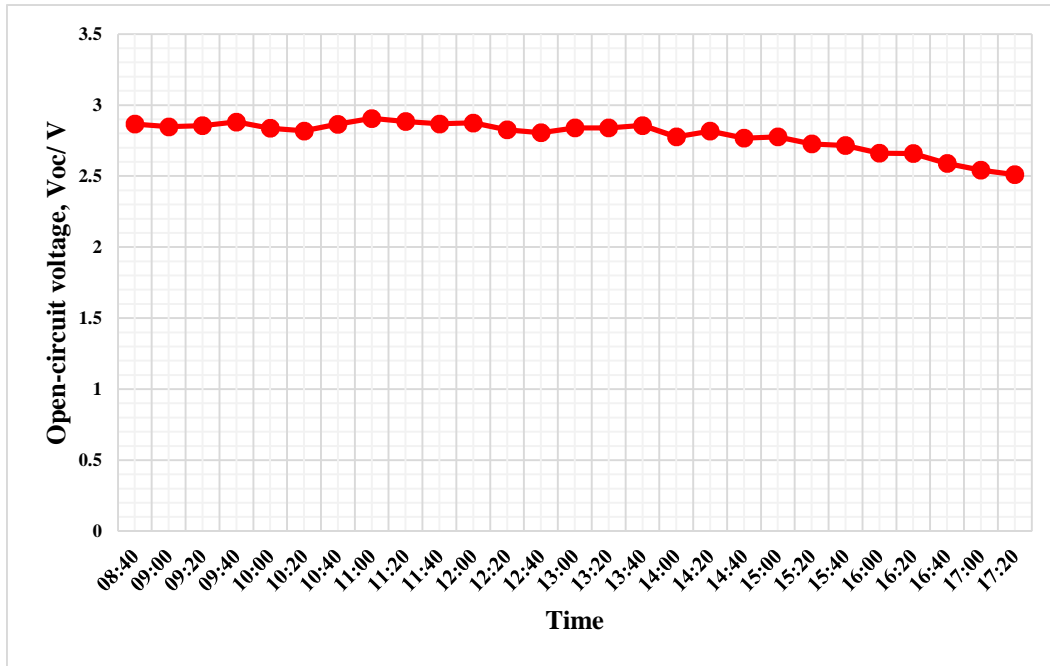


Fig. 13. Open-circuit voltage of the CPV/D module.

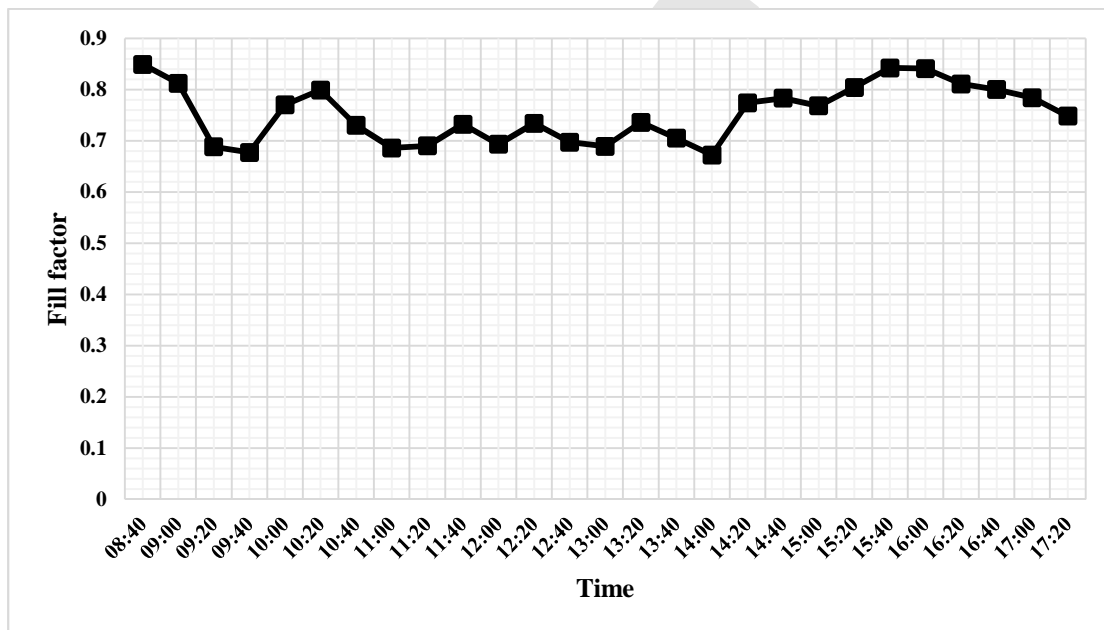


Fig. 14. Fill Factor of the CPV/D module.

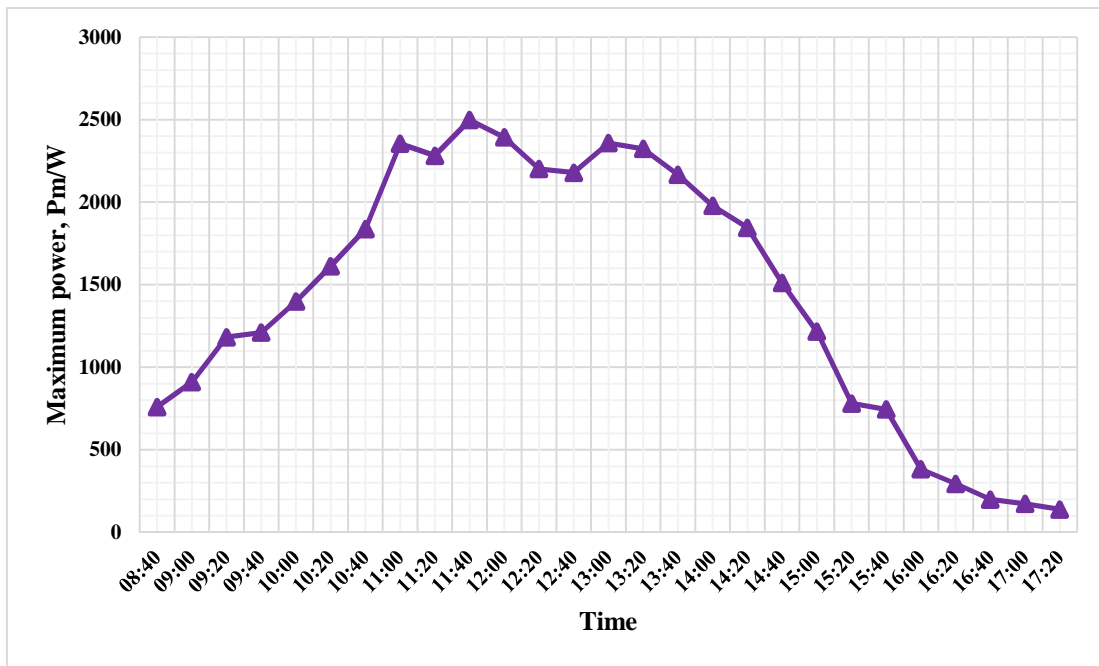


Fig. 15. Maximum power of the CPV/D module.

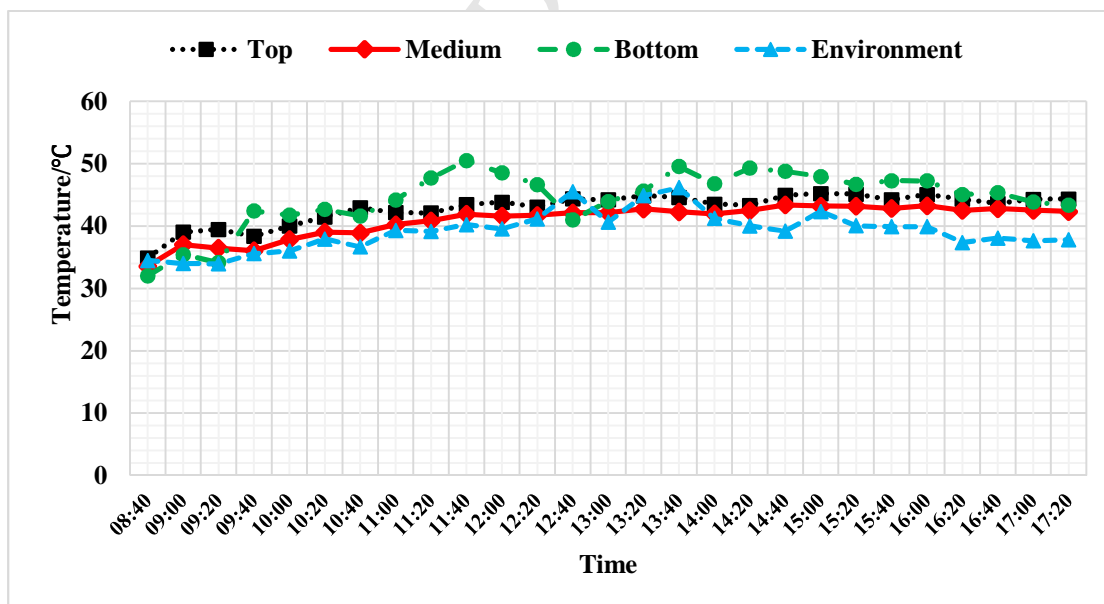


Fig. 16. The temperature of the environment and top, medium, bottom area in the box.

Table captions:

Table 1. Test conditions when the electrical and illumination test are conducted.

Table 2 Cost of the material in the CPV/D window.

ACCEPTED MANUSCRIPT

Table 1 Test conditions when the electrical and illumination test are conducted.

Time	Temperature of the PV panel ($^{\circ}\text{C}$)	Solar radiation intensity (Wm^{-2})	Environment temperature ($^{\circ}\text{C}$)	Wind speed (ms^{-1})
8:40	35.05	470.15	34.50	2.80
9:00	41.73	563.98	34.00	3.00
9:20	40.07	732.48	33.94	4.40
9:40	41.24	797.70	35.58	2.20
10:00	41.64	804.27	35.99	2.50
10:20	43.05	881.82	37.93	3.30
10:40	44.72	922.59	36.66	2.50
11:00	47.77	990.23	39.32	2.20
11:20	51.51	992.66	39.13	1.20
11:40	51.27	1101.33	40.24	3.40
12:00	46.89	932.28	39.53	2.10
12:20	49.37	1143.83	41.17	3.60
12:40	50.48	1019.15	45.51	2.70
13:00	45.64	861.73	40.62	1.30
13:20	50.50	1021.74	44.89	2.30
13:40	49.17	907.78	46.17	3.40
14:00	49.76	880.26	41.23	1.90

14:20	51.62	838.04	40.04	4.20
14:40	50.50	729.47	39.19	2.40
15:00	48.96	650.89	42.34	3.50
15:20	47.97	627.36	40.05	1.70
15:40	50.23	588.85	39.89	2.30
16:00	47.00	520.02	39.91	1.40
16:20	46.16	420.02	37.35	4.20
16:40	45.29	315.32	38.07	1.40
17:00	44.31	259.37	37.65	1.50
17:20	43.53	204.27	37.80	1.30

Table 2 Cost of the material in the CPV/D window.

	Cost of manufacturing (in \$ m ⁻²)	
	3 kWp system	50 MWp system
PMMA and making cost	89.50 (37.00 and 52.50)	37.00
Sylgard	22.00	14.00
Glass	36.75	20.00
Frame	42.00	25.00
PV cell	100.00	59.17
Total	290.25	155.17

Note: the price is evaluated by per square meter of concentrator aperture cover area.

Nomenclature			
BIPV	Building Integrated Photovoltaic	n	diode ideality factor
BAPV	Building Attached Photovoltaic	$Q_{Daylighting}$	the solar radiation for daylighting
C	geometric concentration ratio of the lens-walled CPC	Q_{PV}	the total solar irradiation captured by the PV cell
CPC	Compound Parabolic Concentrator	Q_{Total}	the total incoming solar radiation from the front aperture
CPV/D	Concentrating Photovoltaic/Daylighting	STC	Standard Test Condition
CPV/T/D	Concentrating photovoltaic/Thermal/Daylighting	Greek symbols	
I_{sc} (A)	short circuit current	k	Boltzmann constant
$I_{sc}^{without}$ (A)	short circuit of the non-concentrating PV	β (°)	Inclination angle
I_{sc}^{with} (A)	Short circuit current of the concentrating PV	θ_{NS} (°)	The N-S projected solar altitude angle
P_m (W)	The maximum power	$\eta_{daylighting}$	Daylighting efficiency
q	charge of electron	η_{opt}	Optical efficiency
		$\eta_{opt,ac}$	Actual optical efficiency of the concentrator

Highlights:

- The design of a novel Concentrating Photovoltaic/Daylighting (CPV/D) window based on the lens-walled CPC;
- The prototype of the CPV/D window was manufactured and assembled for the outdoor experiment;
- The overall daylighting and electrical performance of the CPV/D window was investigated under the real weather condition;
- The preliminary economic analysis was made;
- The experiment results prove good daylighting and electrical performance of the CPV/D window.